

# A Comparative Study of Different Image Denoising Methods

Afreen Mulla, A.G.Patil, Sneha Pethkar, Nishigandha Deshmukh

**Abstract**— Image denoising is a serious problem in image processing. Before processing image for further analysis it is important to remove noise from that image. Many denoising algorithms are available but they have their own assumptions, advantages and limitations.

Noise in synthetic images is easily recognised by human eye rather than natural images. Recently, different state of the art methods are proposed for denoising synthetic images. In this paper, comparative analysis of different image denoising methods is done. This paper presents results for natural and synthetic images contaminated with different type of noise.

**Index Terms**— AWGN, bilateral filtering, deterministic annealing, image denoising, robust noise estimation.

## I. INTRODUCTION

In image processing, the classic image denoising problem is the reconstruction of the original image from a noisy image. Noise may get added to the image during acquisition of image or during transport over analog media. Image has been contaminated with *additive white Gaussian noise* (AWGN) is the most common simplifying assumption. It is also assumed that noise is stationary and uncorrelated among pixels and its variance is known.

Recently Knaus and Zwicker demonstrated with dual domain image denoising (DDID) that simple algorithms can achieve high-quality results [1]. DDID combines two methods operating in two different domains i.e spatial domain and frequency domain. This formulation gives better results than used separately.

They extended their work and propose progressive image denoising a method based on robust noise estimation deterministic annealing.

We have approached for quantitative and qualitative analysis of this algorithm for different types of noises like AWGN, Salt & pepper noise, Poisson noise. In this paper, we used two methods i.e Dual domain image denoising (DDID) and Progressive image denoising (PID).

The bilateral filter is known for its edge-preserving properties. It retains high-contrast features like edges, but cannot preserve low-contrast detail like textures without introducing noise. STFT wavelet shrinkage on the other hand

results in good detail preservation, but suffers from ringing artifacts near steep edges. [1]. These two methods are combined to form a new method called DDID. Fig.1 shows the block diagram for DDID.

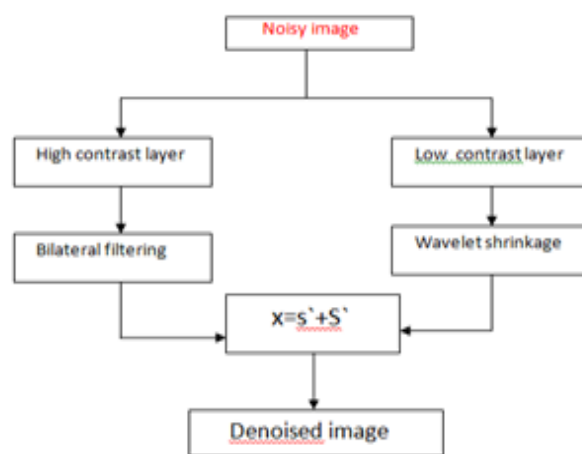


Fig.1 Block diagram for Dual Domain Image Denoising (DDID)

Deterministic annealing is an efficient heuristic method for solving complex optimization where many local extrema exist [3][4]. As like typical high-quality results, void of artifacts are more apparent. The algorithm is usually short fitting into a column of this paper. Finally this formulation using robust estimators and iterative filtering offers opportunities to explore alternative implementations of the image denoising process. Fig. 1 shows the block diagram for Progressive Image Denoising (PID).

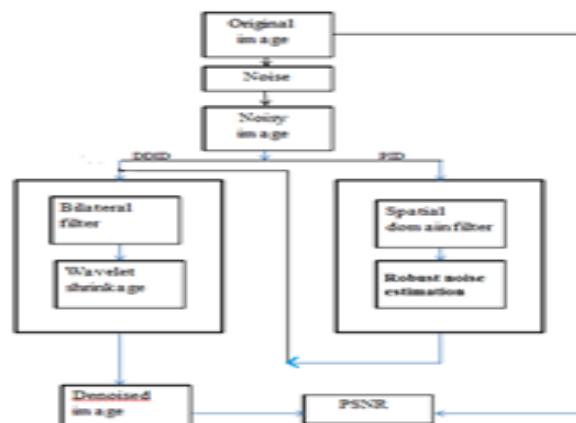


Fig. 2 Block diagram for Progressive Image Denoising (PID)

Later, this paper is organized as follows. The two algorithms of DDID and PID are described in section II,

Manuscript received April 21, 2015.

Afreen Mulla, UG Student, PVPIT, Budhgaon.

A.G.Patil, Associate Professor, PVPIT, Budhgaon

Sneha Pethkar, UG Student, PVPIT, Budhgaon

Nishigandha Deshmukh, UG Student, PVPIT, Budhgaon

followed by implementation details in section III . High Quality results and comparative study for different types of noise is presented in section IV and section V includes the conclusion.

## II. ALGORITHM

In this section we describe the image denoising algorithm based on deterministic annealing & robust noise estimation & which is implemented using a simple iterative filtering scheme.

### A. Progressive Noise Removal

A signal  $O$  has been contaminated with additive white gaussian noise  $n$  and variance  $\sigma^2$ . The task is to decompose the noisy signal  $I$  into its original signal  $O$  and noise  $n$  like.

$$I = O + n . \tag{1}$$

But in practice, we can only estimate a decomposition  $I = \tilde{O} + \tilde{n}$ . Many of the estimation problems are often formulated as energy minimizing problems. Attempt to formulate denoising as a gradient descent with

$$= O_i - \lambda \nabla E(O_i) \tag{2}$$

Starting at  $O_0 = I$ . The scale factor  $\lambda$  controls the step size in the direction of the gradient descent. An attempt to define the energy term as  $E(O_i) = (O_i - O)^2$  fails, since ' $O$ ' is unknown. However, it is empirically discovered that the gradient of this energy,  $\nabla E(O_i)$  can be estimated as a noise estimate  $n_i$  for iteration. Substituting  $\nabla E(O_i) \rightarrow n_i$ , we get.

$$O_{i+1} = O_i - \lambda n_i \tag{3}$$

Allowing us to reinterpret the gradient descent as a progressive removal of noise differentials  $\lambda n_i$ , which integrate over time  $i$  the estimated total noise instance as

$$\tilde{n} = \lambda \sum_{i=0}^{\infty} n_i .$$

### B. Robust Noise Estimation

In order to estimate the noise  $n_i$  for iteration  $i$ , it is necessary to distinguish signal from noise. Hence, conceptually decomposing the noisy signal in three categories: large and medium amplitude signals and medium amplitude noise. Spatial domain can be selected for recognising large amplitude signals. But if the amplitude of the signal is smaller, more similar to the noise, signal and noise cannot be reliably distinguished in the spatial domain. However, the property that signal is autocorrelated and noise is uncorrelated can be utilised. Auto-correlated signals, i.e waves are best detected as large amplitude signals in the frequency domain. Therefore, by using robust estimators to reject large amplitude gradients in spatial domain and medium amplitude gradients in frequency domain, the small amplitude noise is estimated.

Consider pixel  $p$  using pixels  $q$  in a neighborhood window  $N_p$  with window radius  $r$ . We first subtract the center pixel

value  $O_{i,p}$  from all the neighboring pixels  $O_{i,q}$  yielding a "gradient"  $d_{i,p,q}$  as

$$d_{i,p,q} = O_{i,q} - O_{i,p} . \tag{4}$$

With the help of this gradient, two kernels defined to mask out large signals, one is range kernel  $kr$  and another spatial kernel  $ks$ , limiting bias from spatially distant pixels. These two kernels combine to an unnormalized bilateral kernel. Finally, to obtain masked signal in frequency domain  $Fp$ , performing a discrete fourier transform, yielding the fourier coefficients  $D_{i,p,f}$  for frequency  $f$  as

$$D_{i,p,f} = \sum_{q \in N_p} d_{i,p,q} K_r \left( \frac{|d_{i,p,q}|^2}{T_i} \right) * K_s \left( \frac{|q-p|^2}{S_i} \right) e^{-j \frac{2\pi}{2r+1} f(q-p)} \tag{5}$$

To avoid confusion with the time  $i$ , we used here the imaginary number  $j = \sqrt{-1}$ . The variables  $T_i$  and  $S_i$  are scale parameters which we will describe in section II-C.

Again in frequency domain, another range kernel  $K$  is used to mask out large Fourier coefficients  $D_{i,p,f}$  representing fine structures and details. Finally, estimating the noise by taking the center pixel after inverse Fourier transforming the signal. To obtain this value, applying the Fourier slicing theorem and average over all the Fourier coefficients and get

$$n_{i,p} = \frac{1}{(2r+1)^2} \sum_{f \in Fp} D_{i,p,q} K \left( \frac{|D_{i,p,f}|^2}{V_i} \right) \tag{6}$$

where,  $V_i$  is another scale parameter which in this case the variance of the Fourier coefficients  $D_{i,p,f}$  and is given as

$$V_i = \sigma^2 \sum_{q \in N_p} K_r \left( \frac{|d_{i,p,q}|^2}{T_i} \right)^2 K_s \left( \frac{|q-p|^2}{S_i} \right)^2 \tag{7}$$

### C. Shape shifting Estimator

For the dynamic parameterization of the robust noise estimator we define the scale parameters  $T_i$  and  $S_i$  as functions of time  $i$ :

$$T_i = \sigma^2 \gamma_s \alpha^{-i} \tag{8}$$

$$S_i = \sigma_s^2 \gamma_s \alpha^{i/2} \tag{9}$$

The first scale parameter  $T_i$  of the range kernel  $kr$  is our temperature which is reduced over time. We found that an exponential decay of the temperature works best, where  $\alpha-1$  is the rate of this decay.  $\gamma_r$  is a large initial scale factor. The second scale parameter  $S_i$ , however, we let grow. When the temperature  $T_i$  is high, the range kernel  $kr$  covers the entire dynamic range and the spatial kernel  $ks$  should be small to reduce bias from neighbouring pixels in the noise estimation. On the other hand, when the temperature is low, the range

kernel becomes narrow and we require larger spatial support to discern autocorrelated signal with small amplitudes from noise. When the temperature has totally cooled down, the range kernel is a Dirac delta, and the spatial kernel is the constant 1, covering the entire spatial domain. The parameter  $\sigma_2$  is the noise variance of the noisy input  $y$  and  $\sigma_s$  defines a reference standard deviation for the spatial kernel. Similar to the parameter  $\gamma_r$  of the range kernel,  $\gamma_s$  is a small initial scale factor for the scale  $\sigma_s$  of the spatial kernel.

For completeness, we add the algorithm of DDID in this paper. Fig.3 shows flowchart for DDID.

#### A. Spatial domain :Bilateral filter

In the first step, calculate the denoised high-contrast value for a pixel  $p$  using a joint bilateral filter. The joint bilateral filter uses the guide image to filter the noisy image. The bilateral kernel over a square neighborhood window centered around every pixel  $p$  with window radius  $r$  is defined. Since it is needed to guide not only the bilateral filter but also the wavelet shrinkage, filtering both guide and noisy images in parallel and obtain the two denoised high-contrast images.



Fig.3.Flowchart for DDID

#### B. Frequency Domain: Wavelet Shrinkage

In the second step, preparing for the wavelet shrinkage in the transform domain by extracting the low-contrast signals and performing the STFT. The STFT is a discrete Fourier transform (DFT) preceded by multiplication of the signal with a window function to avoid boundary artifacts. When the spatial Gaussian of the bilateral kernel as the window function is chosen, and the entire step becomes a Gabor transform of the low-contrast signal. To transition to the frequency domain, performing a non-unitary DFT.

### III.IMPLEMENTATION

Unlike most other image denoising methods this algorithm is simple enough and a MATLAB implementation for gray scale images is given in this paper.

The formulation of the original DDID uses a wavelet shrinkage kernel in the frequency domain which is replaced by the robust noise estimation in PID.

We used a single real-time image and a computer generated ,synthetic image. Both the images are degraded by adding three types of noise namely, AWGN, Salt & pepper and Poisson noise.

The parameters in the algorithm were empirically found and are the same for all noise levels. We use  $N=30$  with a temperature delay rate of  $\alpha^{-1} = 1.533^{-1}$  & gradient step size  $\lambda=0.567 \log \alpha$ . These parameters change together. The initial scale factor for the range scale is  $\gamma_r=988.5$  and for the spatial scale  $\gamma_s=2/9$ . The window radius is  $r = 15$ , and reference spatial sigma of  $\sigma_s=7$  for the final DDID step, we use a larger kernel size with window radius  $r=31$  and spatial sigma  $\sigma_s=16$ . The range and frequency domain parameters are  $\gamma_r=0.6$  &  $\gamma_s=2.16$ .

The number of iterations  $N$  needs to be large enough to get good denoising results. The gradient descent step factor  $\lambda$  has the effective biggest influence on PSNR. Small values means that the noise will be underestimated & consequently the image will contain residual noise. Conversely, large values means that the noise is over estimated & the image will loose details. The remaining parameters are robust against change & are optimal with tolerance in range of 0.1 dB.

For color images, a 3- point discrete cosine transform. Can be performed on the color channels. The noise variance remain constant& uncorrelated, since DCT is a unitary transformation. For the range kernel definition, the normalized Euclidian distances are averaged independently in frequency domain.

### IV.RESULTS

In this section , we present the results of algorithm for grayscale images.We analyze the denoising process for natural and synthetic images.

Table I and Table II compares the peak signal-to-noise ratio (PSNR) of DDID and PID for same images. We choose  $\sigma= 25$  as the standard deviation of the noise. Numerically, DDID and PID show comparable denoising quality.

We used 30 iterations wherein the PSNR increases fast in beginning and slows down as noise becomes smaller.The corresponding MSE exhibits a strong linear decrease and approach the square bias as the variance .

Table I and II gives evidence that the PID method is superior for the AWGN contaminated images.While DDID gives better results for salt &pepper and poissons noise in lesser time.

For synthetic images, PID reconstructs clean contours and gradients. Numerically, PID is more competitive than DDID when AWGN is added to the synthetic image.

TABLE I

COMPARISON OF PID AND DDID FOR NATURAL IMAGE CONTAMINATED WITH DIFFERENT TYPES OF NOISE.( FOR  $\sigma=25$ ).

Sr.no	Type of Noise Added	DDID PSNR(dB)	PID PSNR(dB)	Time elapsed (sec)	
				DDID	PID
1.	AWGN noise	28.95	<b>29.01</b>	13.72	116.46
2.	Salt & pepper noise	<b>25.38</b>	24.03	12.18	112.01
3.	Poissons noise	30.41	30.13	11.84	115.57

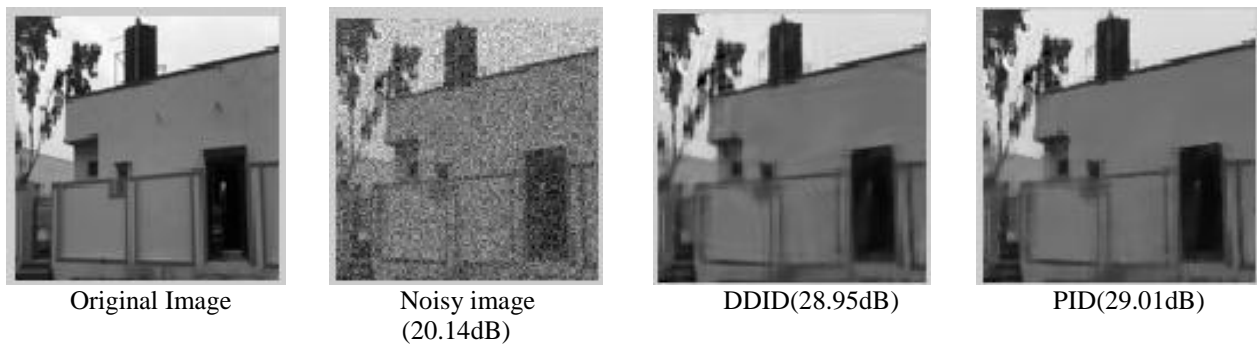


Fig .4 Comparison of PID and DDID for natural image contaminated with AWGN noise.

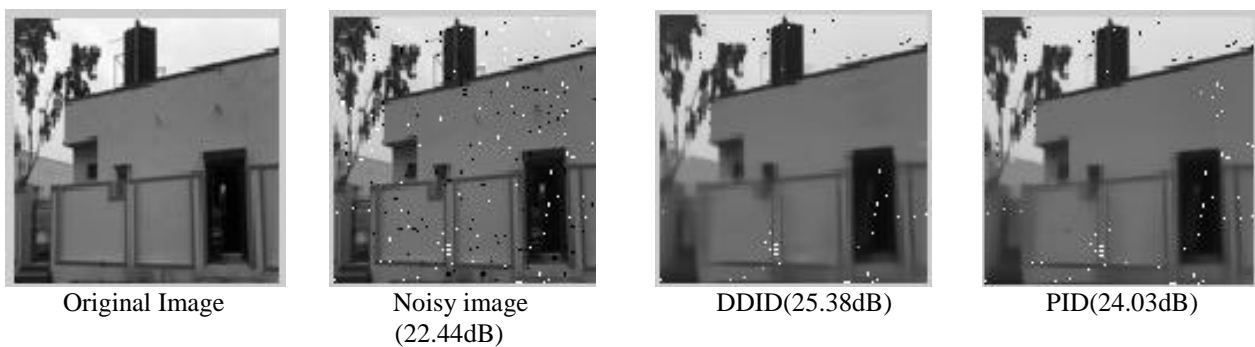


Fig .5 Comparison of PID and DDID for natural image contaminated with Salt & peppers noise.

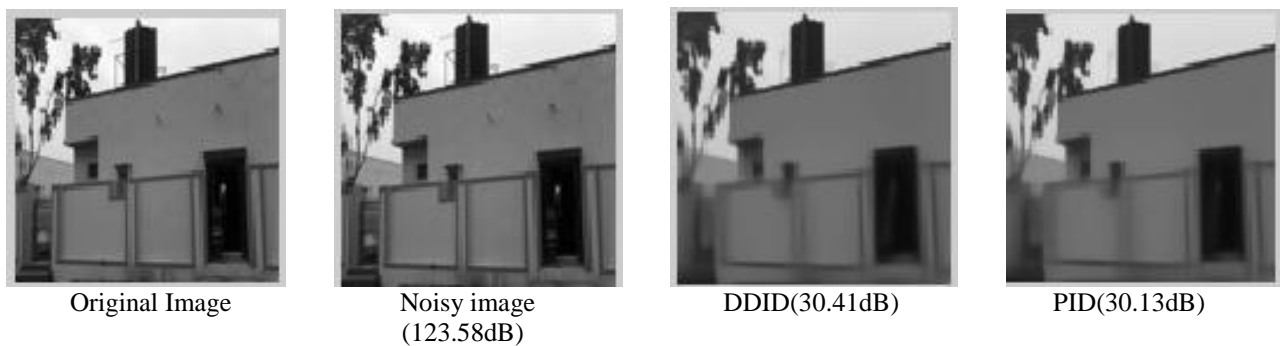


Fig .6 Comparison of PID and DDID for natural image contaminated with Poissons noise

TABLE II

COMPARISON OF PID AND DDID FOR SYNTHETIC IMAGE CONTAMINATED WITH DIFFERENT TYPES OF NOISE.( for  $\sigma=25$ ).

Sr.no	Type of Noise Added	DDID PSNR(dB)	PID PSNR(dB)	Time elapsed (sec)	
				DDID	PID
1.	AWGN noise	30.40	<b>31.26</b>	11.85	111.21
2.	Salt & pepper noise	<b>29.20</b>	27.04	19.67	165.85
3.	Poissons noise	31.60	<b>32.65</b>	17.50	133.60

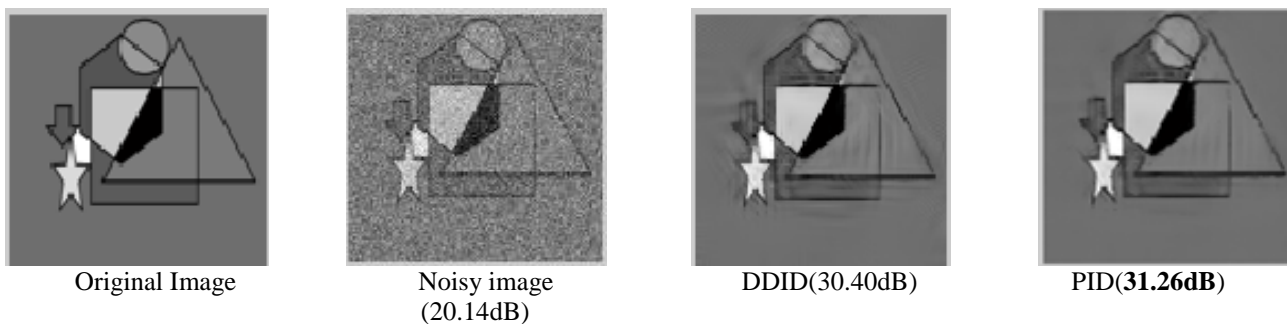


Fig .7 Comparison of PID and DDID for Synthetic image contaminated with AWGN

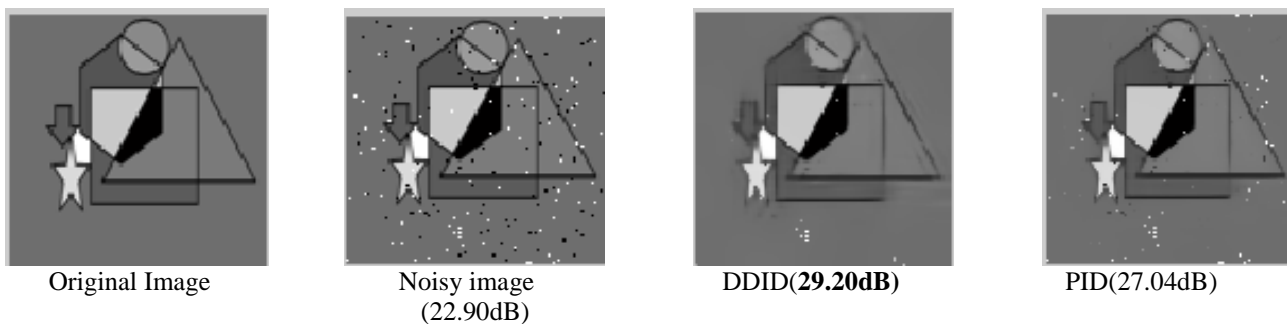


Fig .8 Comparison of PID and DDID for synthetic image contaminated with salt and peppers noise

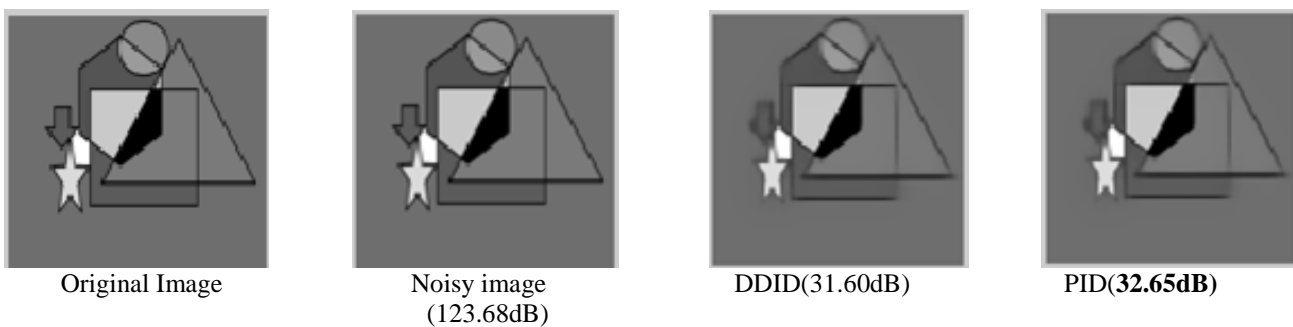


Fig .9 Comparison of PID and DDID for natural image contaminated with Poissons noise

### V.CONCLUSION

In contrast to current state-of-the-art denoising methods, our algorithm is short. Despite its simplicity, the algorithm delivers high-quality results, outperforming other methods in denoising synthetic images. Considering that many methods already work well enough for natural images, the new challenge is in denoising synthetic images contaminated with AWGN.

After analysing PID for different types of noises ,we have came to a conclusion that PID gives excellent visual and theoretical results for synthetic images.

### REFERENCES

- [1] C. Knaus and M. Zwicker, "Dual-domain image denoising," in *Proc. 20th IEEE ICIP*, Sep. 2013, pp. 440–444.
- [2] Claude Knaus, Member, IEEE, and Matthias Zwicker, "Progressive Image Denoising" *IEEE Transaction on Image Processing*, VOL. 23, NO. 7, JULY 2014.
- [3] S. Z. Li, "Robustizing robust M-estimation using deterministic annealing," *Pattern Recognit.*, vol. 29, no. 1, pp. 159–166, Jan. 1996.
- [4] R. Frühwirth and W. Waltenberger, "Redescending m-estimators and deterministic annealing, with applications to robust regression and tail index estimation," *Austrian J. Statist.*, vol. 37, nos. 3–4, pp. 301–317, 2008.
- [5] K. Dabov, A. Foi, V. Katkovnik, and K. Egiazarian, "BM3D image denoising with shape-adaptive principal component analysis," in *Proc. SPARS*, 2009
- [6] Hossein Talebi, Student Member, IEEE, and Peyman Milanfar, Fellow, IEEE "Global Image Denoising" *IEEE Transaction on Image Processing*, VOL. 23, NO. 2, FEBRUARY 2014.
- [7] P. Chatterjee and P. Milanfar, "Is denoising dead?," *IEEE Trans. Image Process.*, vol. 19, no. 4, pp. 895–911, Apr. 2010.
- [8] C. Tomasi and R. Manduchi, "Bilateral filtering for gray and color images," in *ICCV*, 1998, pp. 839–846.
- [9] K. Dabov, A. Foi, V. Katkovnik, and K. Egiazarian, "Image denoising by sparse 3-D transform-domain collaborative filtering," *IEEE Trans. Image Process.*, vol. 16, no. 8, pp. 2080–2095, Aug. 2007.

**Afreen Mulla** is a UG student from Electronics and Telecommunication of PVPIT Budhgaon Her area of interest is in Signals & Systems and Image Processing.

**Mr.A.G.Patil** is working as Associate Professor in Electronics and Telecommunication of PVPIT Budhgaon.His teaching experience is 20 years and area of interest is Image Processing and Digital signal processing.

**Sneha Pethkar** is a UG student from Electronics and Telecommunication of PVPIT Budhgaon Her area of interest in Digital signal processing and Image Processing.

**Nishigandha Deshmukh** is a UG student from Electronics and Telecommunication of PVPIT Budhgaon Her area of interest is in Communication Systems and Image Processing.